Sensors and Actuators B 207 (2015) 90–96

Contents lists available at ScienceDirect

Sensors and Actuators B: Chemical

journal homepage: www.elsevier.com/locate/snb

Electrospun nanofibers of p-type NiO/n-type ZnO heterojunction with different NiO content and its influence on trimethylamine sensing properties

Chao Li[a], Caihui Feng[c], Fengdong Qu[a], Juan Liu[a], Linghui Zhu[a], Ying Lin[a], Ying Wang[a], Feng Li[b], Jingran Zhou[b,*], Shengping Ruan[a,*]

[a] State Key Laboratory on Integrated Optoelectronics, Jilin University, Changchun 130012, PR China
[b] College of Electronic Science and Engineering, Jilin University, Changchun 130012, PR China
[c] College of Instrumentation and Electrical Engineering, Jilin University, Changchun 130012, PR China

ARTICLE INFO

Article history:
Received 30 May 2014
Received in revised form 8 October 2014
Accepted 8 October 2014
Available online 16 October 2014

Keywords:
ZnO
NiO
Heterojunction
Nanofibers
Trimethylamine sensor

ABSTRACT

Nanofibers of p-type NiO/n-type ZnO heterojunction with different NiO content were fabricated by a facile electrospinning technique. The as-synthesized nanofibers were characterized by differential thermal analyzer (DTA) and thermal gravimetric analyzer (TGA), X-ray diffractometer (XRD), scanning electron microscopy (SEM) and transmission electron microscopy (TEM). The p–n junction formed between cubic NiO particle and hexangular ZnO particle in the NiO/ZnO nanofibers was confirmed and highly improved the trimethylamine (TMA) sensing properties. The influence of NiO content in nanofibers on TMA sensing properties was studied. The results showed that the NiO/ZnO nanofibers exhibited the significantly enhanced response, good selectivity, fast response and recovery rate (less than 30 s and 35 s, respectively), and excellent linearity (in a relatively wide range of 0.5–200 ppm). Especially, the NiO/ZnO nanofibers with 4 mol% of NiO has the best performance, whose response to 100 ppm TMA could reach 892 and detection limit could extend down to 0.5 ppm at 260 °C. The mechanism of the enhanced TMA sensing performance caused by p-type NiO/n-type ZnO heterojunctions in the NiO/ZnO nanofibers was also discussed.

1. Introduction

With the improvement of people's life, seafood as an indispensable source of biologically valuable proteins, fats and fat-soluble vitamins, are extensively consumed all over the world. Consumption of spoiled seafood could cause serious health problems, such as septicemia and gastroenteritis, so detecting the freshness of seafood becomes a necessity in food industry [1]. Many research have shown that trimethylamine (TMA) can be used as an effective indicator of seafood quality because its content is increased with the decomposition of trimethyl-N-oxide in seafood after death [2–4]. In the evaluation of fish freshness, 0–10 ppm is regarded as fresh, and decay begins at over 10 ppm of TMA [5]. TMA as a malodorous gas existing in living or working environment is often released from fish-meal manufacturing process, wastewater treatment, waste disposal landfills, livestock farming, and hog manure [6]. Due to its potentially toxic and likely carcinogenic properties, TMA is considered as a strong environmental pollutant. TMA can irritate people's eyes and respiratory systems and has also been reported to inhibit the synthesis of macromolecules such as DNA, RNA and proteins and to have a teratogenic effect on animal embryos [7]. TMA is also observed in human exhaled breath as a result of an imbalance in the renal organ system and thus serves as the biomarker of renal diseases [8].

So far, plenty of methods such as gas sensory evaluation, pH test, chromatography, high performance liquid chromatography, ion mobility spectrometry, and mass spectrometry etc., have been explored to analyze the content of TMA. However, among these methods, problems such as lack of accuracy, requires of complicated equipment, long sample preparation time, and professional operating skills are still difficult to overcome [2]. In contrast, gas sensors based on oxide semiconductors like ZnO, WO_3, SnO_2, MoO_3, In_2O_3, etc., make it possible to realize cost-effective, rapid, reliable, nondestructive, on-site and real-time TMA analyzing [2,3,5,9–13].

As an important semiconductor material, ZnO is widely used as a kind of gas sensing material due to its biocompatibility,

* Corresponding authors. Tel.: +86 431 85168242; fax: +86 431 85168242.
E-mail addresses: zhoujr@jlu.edu.cn (J. Zhou), ruansp@jlu.edu.cn (S. Ruan).

http://dx.doi.org/10.1016/j.snb.2014.10.035
0925-4005/

nontoxicity, stability, low-cost, ease of large scale fabrication and superior sensing properties [14–18]. In early years, Tae-Ha Kwon etc. reported the effects of dopants, film thickness and heat treatment on TMA sensing properties of ZnO-based film, and the sensitivity of the sensor could reach 350, and 13–160 ppm and 2 ppm TMA at 300 °C, respectively [19]. SnO_2—ZnO nanocomposite sensor fabricated by Zhang etc. showed high sensitivity and excellent response/recovery characteristics in the range of 1–500 ppm TMA as well as good selectivity and stability [20]. Gas sensors based on polyvinylpyrrolidone (PVP)-modified ZnO nano-particles with a molar ratio of Zn^{2+}:PVP = 5:5 exhibited fairly excellent sensitivity and selectivity [9].

In recent years, heterojunction reported by plenty of research can effectively improve properties of materials, which have been a focus of current nanoscience and nanotechnology and have led to growing interest in the field of ultraviolet detection, catalysis, solar cell, laser and other applications [21–28]. For example, TiO_2@ZnO n–p–n heterojunction nanorod prepared by Lin et al. via a hydrothermal method, could worked more efficiently as photocatalysts in comparison to bare ZnO nanorods and TiO_2 nanoparticles [29]; SnO_2@TiO_2 heterojunction nanostructures prepared by Hou et al. exhibited a high photocurrent, excellent self-powered, fast response and "visible blind" characteristics as the active material of photoelectrochemical UV detectors [30]. ZnO/α-Fe_2O_3 hierarchical nanostructures synthesized by Huang and Fan exhibited a much higher sensitivity to ethanol vapor than the pure ZnO [31].

In this paper, nanofibers of pure ZnO and p-type NiO/n-type ZnO heterojunction were fabricated through an electrospinning method and calcination technique. The influence caused by different NiO content on the TMA sensing properties was investigated. NiO/ZnO heterojunction efficiently improving TMA sensing properties of ZnO nanofibers, such as higher response, lower detect limit and better selectivity was observed and the possible mechanism was also discussed.

2. Materials and methods

2.1. Chemical reagents

All the starting materials (AR grade): zinc acetate ($Zn(CH_3COO)_2{\cdot}4.5H_2O$), nickel chloride ($NiCl_2{\cdot}6H_2O$), and polyvinyl pyrrolidone (PVP, Mw ≈ 1,300,000) were purchased from the Sinopharm Chemical Reagent Co. Ltd., and used as received without any further purification.

2.2. Preparation of nanofibers of p-type NiO/n-type ZnO heterojunction

In a typical procedure, nanofibers of p-type NiO/n-type ZnO heterojunction were synthesized using an electrospinning and calcination method. It is described as follows: first, 0.4 g of $NiCl_2{\cdot}6H_2O$ and $Zn(CH_3COO)_2{\cdot}4.5H_2O$ with certain ratio were dissolved in 8.8 g mixed solution containing N,N-dimethylformamide (DMF)/ethanol (EtOH) weight ratio of 1:1 and stirred for 2 h. Subsequently, 0.8 g of polyvinyl pyrrolidone (PVP, Mw = 1,300,000) was added to the above solution. After stirring at room temperature for 6 h, the precursor solution of the PVP/$NiCl_2$/$Zn(CH_3COO)_2$ composite was obtained. Subsequently, the above precursor solutions were drawn into a plastic syringe and connected to anode of a variable high-voltage power supply. A voltage of 20 kV was applied between the cathode (a flat aluminum foil as the collector) and the anode (syringe tip) at a distance of 20 cm to prepare PVP/$NiCl_2$/$Zn(CH_3COO)_2$ composite fibers. Afterward, the above composite nanofibers were calcined at a rate of 1 °C/min and remained for 2 h at 600 °C. Thus, nanofibers of p-type NiO/n-type ZnO heterojunction with 2, 4, 6, 8 and 10 mol% of NiO (denoted as NZ-2, NZ-4, NZ-6, NZ-8 and NZ-10 nanofibers, respectively) were successfully prepared, respectively. Moreover, to investigate the structure and gas sensing properties of NiO/ZnO nanofibers, pure ZnO nanofibers were prepared using the same experimental conditions.

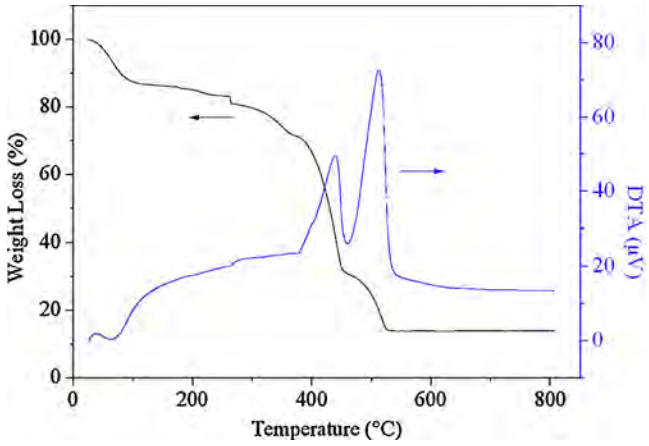

Fig. 1. DTA–TGA curves of the $Zn(CH_3COO)_2$/PVP/$Ni(CH_3COO)_2$ composite nanofibers.

2.3. Characterization

The nanofibers were characterized by differential thermal analyzer (DTA) and thermal gravimetric analyzer (TGA) (Melttler Toledo 825^e), X-ray diffractometer (XRD) (Shimadzu XRD-6000, Cu Kα radiation), scanning electron microscopy (SEM) (XL30 ESEM FEG) and transmission electron microscopy (TEM) (TECNAI G2).

2.4. Fabrication and measurement of sensors

The fabricating process of sensors in brief: The as-prepared nanofibers were mixed with deionized water in a weight ratio of 100:25 to form a paste. The paste was coated onto a ceramic tube on which a pair of gold electrodes was previously printed, and then a Ni–Cr heating wire was inserted in the tube to form a side-heated gas sensor [32].

Gas sensing properties were measured by a chemical gas sensor-8 (CGS-8) intelligent gas sensing analysis system (Beijing Elite Tech Co. Ltd., China) [32]. The gas response was defined as $S = R_a/R_g$, where the R_g and R_a are the resistance values of sensors in the presence and absence of the target gas, respectively. The time taken by the sensor to achieve 90% of the total resistance change was defined as the response time in the case of adsorption or the recovery time in the case of desorption.

3. Results and discussion

3.1. Characterization

The DTA–TGA curves of the as-electrospun PVP/$NiCl_2$/$Zn(CH_3COO)_2$ composite nanofibers are shown in Fig. 1. It is clear from the TGA curve that all the volatile (H_2O and ethanol), organic components (PVP, DMF), CH_3COO^- groups and Cl^- were removed completely below 550 °C, which resulted in a metal oxide phase. Moreover, the DTA curve exhibits two obvious exothermic peaks at 439.7 and 512.9 °C respectively and they correspond to about 52.6% weight loss. This significant weight loss was attributed to the oxidation of $Zn(CH_3COO)_2$ and $NiCl_2$, and the degradation

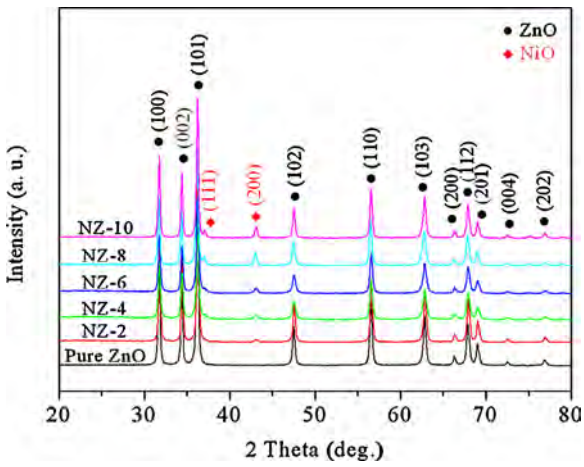

Fig. 2. XRD patterns of the pure ZnO and NiO/ZnO nanofibers.

of PVP, which involved both intra- and intermolecular transfer reactions, and the burning out of organic composites. The minor weight loss before 127.2 °C corresponds to the removal of the residual solvent and water in the composite nanofibers and the total weight-loss evaluated by TGA is about 86.08% in the heating process. According to the DTA–TGA analyses mentioned above, the following sintering temperature is chosen at 600 °C.

Fig. 2 shows the XRD patterns of pure ZnO, NZ-2, NZ-4, NZ-6, NZ-8 and NZ-10 nanofibers. It can be seen that the diffraction patterns at $2\theta = 31.8°$, 34.4°, 36.2°, 47.5°, 56.6°, 62.9°, 66.3°, 68°, 69.1°, 72.5° and 76.9° correspond to (1 0 0), (0 0 2), (1 0 1), (1 0 2), (1 1 0), (1 0 3), (2 0 0), (1 1 2), (2 0 1), (0 0 4), and (2 0 2) characteristic peaks of hexagonal wurtzite ZnO (JCPDS: 36-1451), respectively. Compared with pure ZnO nanofibers, the presence of diffraction peaks at 37.3° and 43.3° for NiO/ZnO nanofibers can be indexed to (1 1 1) and (2 0 0) crystal lattice planes of cubic phase NiO (JCPDF: 78-0643), indicating that NiO nanoparticles separated from the ZnO nanoparticles and formed NiO/ZnO heterojunction due to the low lattice mismatch between NiO and ZnO [27]. In addition, no other characteristic peaks for impurity are observed.

The SEM images of the as-electrospun composite nanofibers after calcination are shown in Fig. 3(a)–(e). It can be seen that, after removing of PVP, ZnO nanofibers with rough surfaces were less than 100 nm in average diameter and up to several microns in length. The bi-modal pore size distribution morphology, formed by micropores among nanofibers and nano-sized pores between nanocrystallites, can facilitate the diffusion and distribution of surrounding gas phase to the surface of the internal nanoparticles, which will increase the reaction sites and contribute to improving the gas sensing properties greatly.

In order to observe the microstructure of the as-electrospun NiO/ZnO nanofibers, high-resolution transmission electron microscopy (HRTEM) were carried out. Fig. 4 shows the representative TEM images of the NZ-4 nanofibers. The low-magnification TEM image of the NZ-4 nanofibers is displayed in Fig. 4(a). It can be seen that the NZ-4 nanofibers are composed of nanoparticles, and each nanoparticle attached to several other nanoparticles. Meanwhile, a high-resolution image shown in Fig. 4(b) reveals the simultaneous presence of the crystalline NiO and ZnO crystal lattices in the NZ-4 nanofibers. The interplanar distances of 0.209 nm are close to the *d* spacings of the (2 0 0) planes of the cubic structured NiO. The interplanar distances of 0.248 nm are close to the *d* spacings of the (1 0 1) planes of the hexagonal structured ZnO. Moreover, a continuity of lattice fringes between the NiO and ZnO nanoparticles can be observed in Fig. 4(b), suggesting that the p–n heterojunction might be formed between the NiO and ZnO nanoparticles in the NiO/ZnO nanofibers.

3.2. Gas sensing properties

In order to find the optimum operating temperature of the sensors, the responses of pure ZnO and NiO/ZnO nanofibers to 100 ppm TMA at different operating temperature (from 110 to 360 °C) were collected. As shown in Fig. 5(a), the response of sensors to TMA increased with the augment of operating temperatures and attained the maximum values at a certain value, followed by a decrease. Remarkably, among all the samples, NZ-4 nanofibers exhibited the highest response of about 892–100 ppm TMA at about 260 °C, which was about nine times as high as that of pure ZnO nanofibers at its optimal operating temperature. The other NiO/ZnO nanofibers also exhibited higher response than the pure ZnO nanofibers at their optimal operating temperature, indicating the p-type NiO/n-type ZnO heterojunction were benefit to TMA sensitivity. All the TMA sensing performances of the samples were investigated under their optimal temperature hereinafter.

In addition, the dependence between response (to 100 ppm TMA) and NiO content of the nanofibers is displayed in Fig. 5(b). As it can be seen, the response intensively depended on the molar percentage of NiO in nanofibers: the response increased dramatically with the increase of NiO content and achieved the highest when NiO content was 4 mol%, then gradually dropped down with the further increase in NiO content. Predictably, according to Fig. 5b, when NiO content surpasses 10 mol% the response of NiO/ZnO nanofibers will decrease further and be even below the pure ZnO nanofibers' response to TMA eventually (in fact, NiO is far less sensitive than ZnO).

The responses of the pure ZnO and NiO/ZnO nanofibers to different concentrations of TMA at optimal operating temperature are shown in Fig. 6. From Fig. 6(a) it can be easily find that the response increased rapidly with the increase in TMA concentration, and then gradually slowed down, but did not reach saturation until 50,000 ppm. Moreover, the NiO/ZnO nanofibers exhibited higher response values than that of pure ZnO nanofibers in the whole testing range. Especially, the NZ-4 nanofibers had the highest response to each concentration of TMA and could detect TMA down to about 0.5 ppm (the response was about 2.9), as shown in Fig. 6(b), which was much higher than the pure ZnO nanofibers (the response was 1.1–0.5 ppm TMA). For TMA at levels of 0.5, 1, 5, 10, 20, 50, 100, and 200 ppm, the response were about 2.9, 5.7, 40, 76, 168, 539, 892 and 1448 for NZ-4 nanofibers and 2.3, 4.5, 24, 54, 110, 296, 593 and 1145 for NZ-2 nanofibers, respectively. Although, the response just lower than NZ-4 nanofibers among all the samples, NZ-2 nanofibers had a better linear detecting range for 0.5–200 ppm TMA.

As for gas sensing applications, rapid response and recovery is of great importance. To investigate the response–recovery behaviors of pure ZnO and NiO/ZnO nanofibers, the sensors were sequentially exposed to 5, 10, 20, 50 and 100 ppm TMA at their optimal operating temperature, respectively. As shown in Fig. 7, when sensors exposed to TMA the response increases rapidly and when subjected to air the sensors' recovery to the initial state were also rapid. The response time and recovery time were within 30 s and 35 s, respectively.

A comparison within our work and with other TMA sensitive materials is displayed in Table 1. It can be seen, NiO/ZnO nanofibers, especially NZ-2 and NZ-4 nanofibers, have an advantage of detecting TMA gas due to the high response, low detectable limit and fast response and recovery rate. It is worth noticed that, with the increase in NiO content, response and recovery time have a light increase while an increase in response to 100 ppm and a reduce in detectable limit.

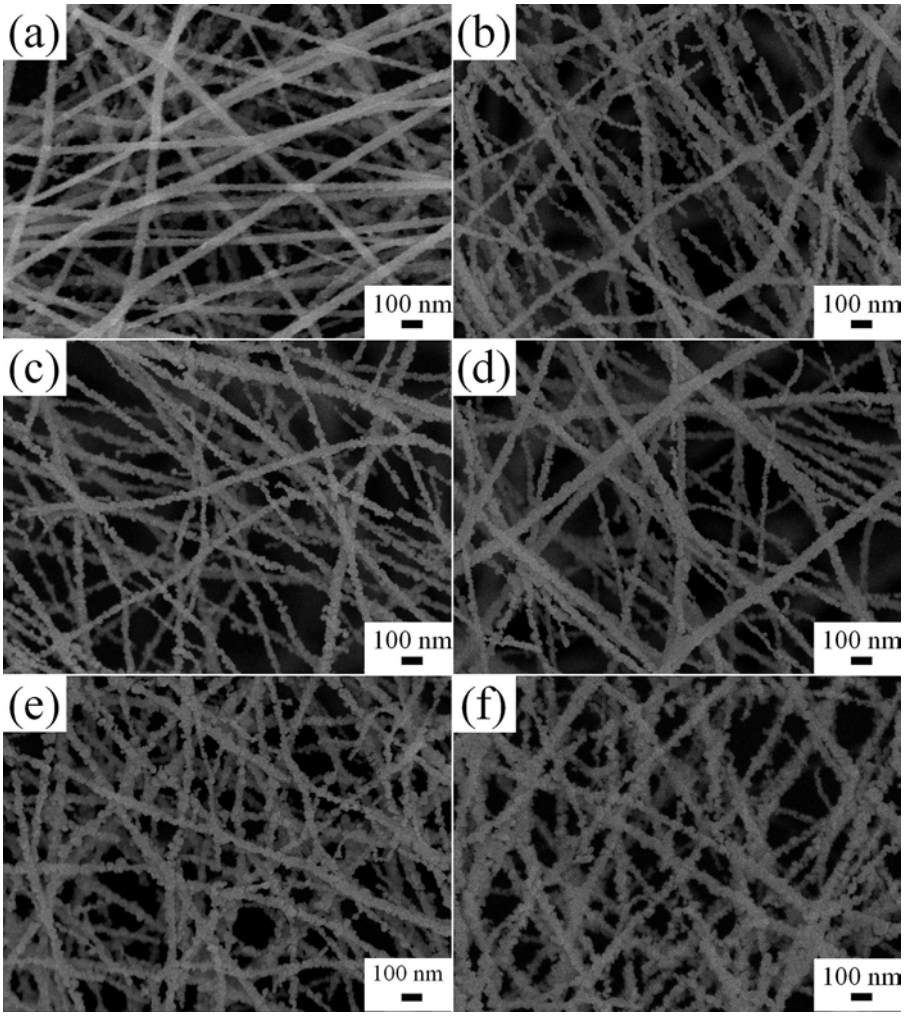

Fig. 3. SEM images of the pure ZnO and NiO/ZnO nanofibers: (a) pure ZnO, (b) NZ-2, (c) NZ-4, (d) NZ-6, (e) NZ-8, (f) NZ-10.

The gas sensing selectivity is another important parameter to evaluate the sensing ability of sensor. The response of ZnO nanofibers and NiO/ZnO nanofibers to 100 ppm TMA, ethanol, ammonia, acetone and methanal at their optimal operating temperature are shown in Fig. 8. As can be seen in this figure, NiO/ZnO nanofibers, especially the NZ-4 ones, had the much higher response to TMA than that to ethanol, ammonia, acetone and methanal compared with the ZnO nanofibers, indicating the better selectivity of NiO/ZnO nanofibers to TMA.

Stability is a key quality indicator in the development of gas sensors for real markets and influenced by many factors [37]. Fig. 9 shows the stability measurements of NZ-4 nanofibers to 100 ppm

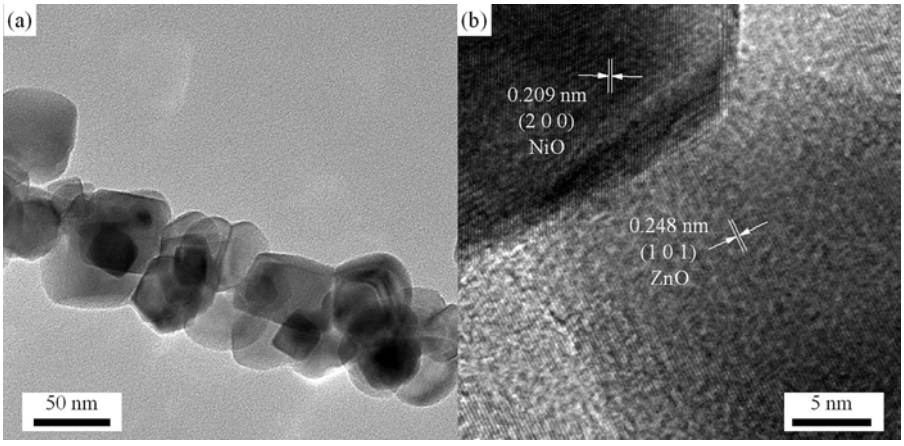

Fig. 4. (a) TEM and (b) HRTEM images of p-type NiO/n-type ZnO heterojunction in NZ-4 nanofibers.

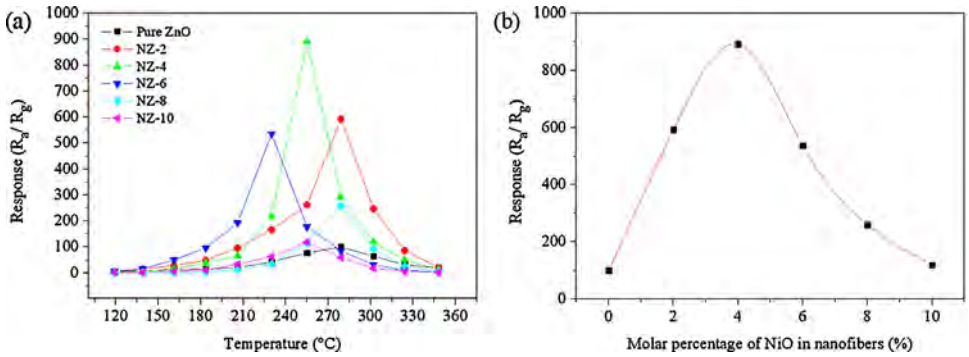

Fig. 5. (a) Response of the pure ZnO and NiO/ZnO nanofibers to 100 ppm TMA measured at different operating temperature and (b) response to 100 ppm versus NiO content of nanofibers.

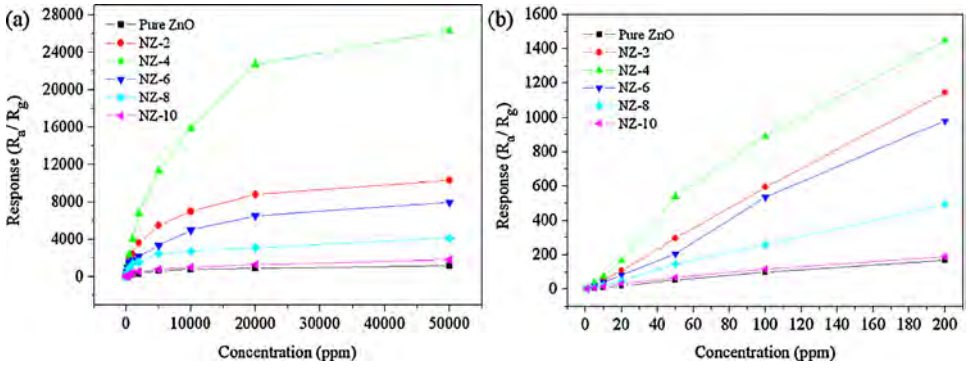

Fig. 6. Response of the pure ZnO and NiO/ZnO nanofibers versus TMA concentrations: (a) 0.5–50000 ppm; (b) 0.5–200 ppm.

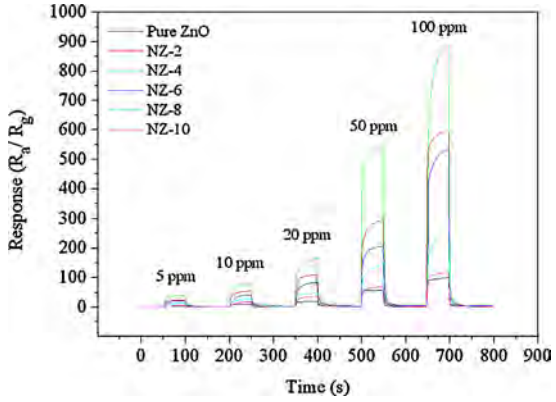

Fig. 7. Real-time response curves of the pure ZnO and NiO/ZnO nanofibers to TMA in the range of 5–100 ppm at their optimal operating temperature.

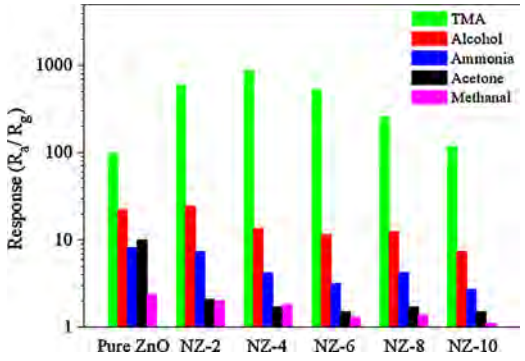

Fig. 8. Selectivity and stability of the pure ZnO and NiO/ZnO nanofibers exposed to 100 ppm target gases at their optimal operating temperature.

Table 1
Sensing properties of some reported TMA-sensitive oxide semiconductor and NiO/ZnO nanofibers.

Materials	TMA concentration (ppm)	Response (R_a/R_g)	Response time	Recovery time	Detectable limit (ppm)
Thoria-incorporated SnO_2 [33]	800	1500	15 s	20 min	–
SnO_2–ZnO nanocomposite [34]	50	92	2 s	100 s	–
CdO–Fe_2O_3 [35]	1000	1527	70 s	170 s	1
WO_3 [10]	100	~15	3.5 s	21 s	50
Flowerlike In_2O_3 [36]	5	~6.2	5 s	10 s	~2
Our work					
Pure ZnO	100		5 s	13 s	5
NZ-2		593	5 s	16 s	1
NZ-4		892	18 s	20 s	0.5
NZ-2		537	16 s	17 s	1
NZ-4		259	26 s	19 s	2
NZ-10		118	12 s	27 s	2

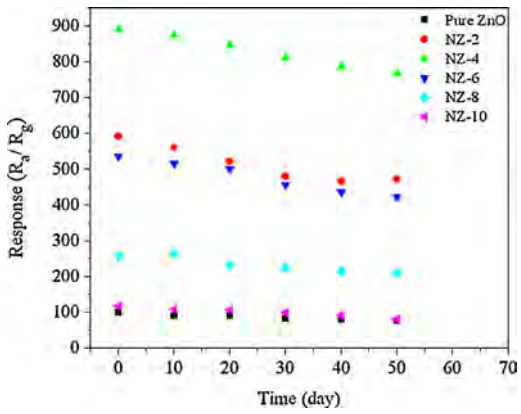

Fig. 9. Stability measurement of NiO/ZnO nanofibers to 100 ppm TMA within 50 days.

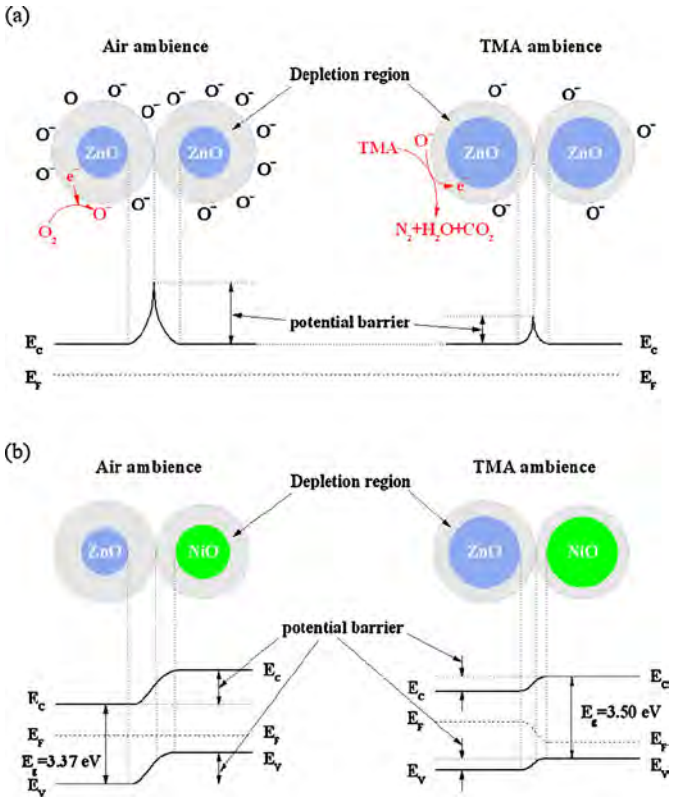

Fig. 10. Schematic diagrams of the TMA sensitive mechanism of pure ZnO and NiO/ZnO nanofibers.

TMA performed within 50 days. The results indicate the sensitivity of the sensors decreased over time, but their responses still have high values.

3.3. Gas sensing mechanism

The TMA sensing mechanism of ZnO nanofibers can be explained as follows and illustrated in Fig. 10(a). Response of semiconducting metal oxides is based on the reactions between target gas molecule and the oxygen species on the surface of oxides [32,38]. When ZnO nanofibers are surrounded by air, oxygen molecules can be adsorbed on their surface to generate chemisorbed oxygen species, which can lead to a decrease in fiber conductive. When the sensor is exposed to TMA, TMA molecules can react with the chemisorbed oxygen species (O^- is believed to be dominant at sensor's operating temperature [39,40]) and the trapped electrons are released back to the conduction band, which will increase the carrier concentration and result in a decrease in the fiber resistance. The reaction between surface oxygen species and TMA can be simply described as [4]:

$$N(CH_3)_3 + 21O^- = N_2 + 9H_2O + 6CO_2 + 42e^- \quad (1)$$

The heterojunction is considered as an important reason for the dramatically enhanced sensitivity of heterostructure materials [5]. It is generally considered that the formation of p–n junctions can decrease sensor' conductivity and increase the barrier height, which are responsible for the enhanced sensor response [41–44]. According to the XRD and TEM analysis mentioned above, it is reasonable to consider p-type NiO nanoparticles disperse in NiO/ZnO nanofibers and thus many p–n junctions are generated near the interface between NiO and ZnO nanoparticles. As shown in Fig. 10(b), because the electrons transfer from n-type ZnO to p-type NiO while the holes transfer from NiO to ZnO until the system obtains equalization at the Fermi level, the wide depletion regions are generated leading to a remarkable decrease in conductivity. In NiO/ZnO nanofibers, the conductivity is dominated jointly by the NiO–ZnO p–n heterojunction barriers and the ZnO–ZnO Schottkey barriers. When the NiO/ZnO nanofibers are exposed to reductive TMA, the electrons trapped by absorbed oxygen species and NiO nanoparticles are feed back to ZnO through surface interactions, which will shrink p–n junction depletion regions and decrease the barrier height. As a result, the conducting channel will be widened and the conductivity could increase significantly. Therefore, the sensor response is remarkably improved.

4. Conclusions

In summary, nanofibers of p-type NiO/n-type ZnO heterojunction with different NiO content were synthesized via electrospinning and calcination, and their TMA sensing performances were analyzed. The results showed that the sensitivity of nanofibers of p-type NiO/n-type ZnO heterojunction to TMA intensively depended on the NiO content. NiO/ZnO nanofibers exhibited not only enhanced response, but also rapid response and recovery rate (less than 30 s and 35 s, respectively), good linearity and selectivity against TMA. Especially, for the NZ-4 nanofibers, the response to 100 ppm TMA could reach 892 (about nine times as high as the pure ZnO ones) and the detection limit could extend down to 0.5 ppm. In addition, despite lower response than NZ-4 nanofibers, NZ-2 nanofibers showed a better linear detecting range for 0.5–200 ppm TMA as well as the second-highest response. Also, the possible sensing mechanism of NiO/ZnO nanofibers on TMA properties was discussed. The excellent properties make NiO/ZnO nanofibers a promising candidate for practical TMA sensing applications.

Acknowledgements

This research is financially supported by the National Natural Science Foundation of China (61274068 and 61275035), Jilin Provincial Science and Technology Department (20120324 and 20130206021GX), and Chinese National Programs for High Technology Research and Development (No. 2009AA03Z402).

References

[1] I.N.A. Ashiea, J.P. Smitha, B.K. Simpsona, D.N.F. Haardb, Spoilage and shelf-life extension of fresh fish and shellfish, Crit. Rev. Food Sci. Nutr. 36 (1996) 87–121.
[2] J.Y. Jung, C.S. Lee, Characteristics of the TiO_2/SnO_2 thick film semiconductor gas sensor to determine fish freshness, J. Ind. Eng. Chem. 17 (2011) 237–242.

[3] X.F. Chu, S.M. Liang, W.Q. Sun, W.B. Zhang, T.Y. Chen, Q.F. Zhang, Trimethylamine sensing properties of sensors based on MoO_3 microrods, Sens. Actuators B: Chem. 148 (2010) 399–403.
[4] X. Chu, S. Zhou, W. Zhang, H. Shui, Trimethylamine sensing properties of nano-$LaFeO_3$ prepared using solid-state reaction in the presence of PEG400, Mater. Sci. Eng. B 164 (2009) 65–69.
[5] H.S. Woo, C.W. Na, I.D. Kim, J.H. Lee, Highly sensitive and selective trimethylamine sensor using one-dimensional ZnO—Cr_2O_3 hetero-nanostructures, Nanotechnology 23 (245501) (2012) 10.
[6] Y. Ding, J.Y. Shi, W.X. Wu, J. Yin, Y.X. Chen, Trimethylamine (TMA) biofiltration and transformation in biofilters, J. Hazard. Mater. 143 (2007) 341–348.
[7] I. Guest, D.R. Varma, Teratogenic and macromolecular synthesis inhibitory effects of trimethylamine on mouse embryos in culture, J. Toxicol. Environ. Health 36 (1992) 27–41.
[8] R. Pandeeswari, B.G. Jeyaprakash, Nanostructured α-MoO_3 thin film as a highly selective TMA sensor, Biosens. Bioelectron. 53 (2014) 182–186.
[9] H.X. Tang, M. Yan, X.F. Ma, H. Zhang, M. Wang, D.R. Yang, Gas sensing behavior of polyvinylpyrrolidone-modified ZnO nanoparticles for trimethylamine, Sens. Actuators B: Chem. 113 (2006) 324–328.
[10] M. Tong, G. Dai, D. Gao, WO_3 thin film sensor prepared by sol–gel technique and its low-temperature sensing properties to trimethylamine, Mater. Chem. Phys. 69 (2001) 176–179.
[11] S.G. Zhao, P.G. Wei, S.H. Chen, Enhancement of trimethylamine sensitivity of MOCVD-SnO_2 thin film gas sensor by thorium, Sens. Actuators B: Chem. 62 (2000) 117–120.
[12] J. Zheng, G. Li, X. Ma, Y. Wang, G. Wu, Y. Cheng, Polyaniline–TiO_2 nanocomposite-based trimethylamine QCM sensor and its thermal behavior studies, Sens. Actuators B: Chem. 133 (2008) 374–380.
[13] X.F. Lu, Q.Y. Yu, K. Wang, L.C. Shi, X. Liu, A.G. Qiu, L. Wang, D.L. Cui, Synthesis, characterization and gas sensing properties of flowerlike In_2O_3 composed of microrods, Cryst. Res. Technol. 45 (2010) 557–561.
[14] M.W. Ahn, K.S. Park, J.H. Heo, J.G. Park, D.W. Kim, K.J. Choi, J.H. Lee, S.H. Hong, Gas sensing properties of defect-controlled ZnO-nanowire gas sensor, Appl. Phys. Lett. 93 (2008) 1–3.
[15] H.S. Al-Salman, M.J. Abdullah, N. Al-Hardan, ZnO thin film nanostructures for hydrogen gas sensing applications, Ceram. Int. 39 (2013) S447–S450.
[16] L. Liu, S. Li, J. Zhuang, L. Wang, J. Zhang, H. Li, Z. Liu, Y. Han, X. Jiang, P. Zhang, Improved selective acetone sensing properties of Co-doped ZnO nanofibers by electrospinning, Sens. Actuators B: Chem. 155 (2011) 782–788.
[17] C.S. Prajapati, P.P. Sahay, Alcohol-sensing characteristics of spray deposited ZnO nano-particle thin films, Sens. Actuators B: Chem. 160 (2011) 1043–1049.
[18] Y. Zeng, Z. Lou, L. Wang, B. Zou, T. Zhang, W. Zheng, G. Zou, Enhanced ammonia sensing performances of Pd-sensitized flowerlike ZnO nanostructure, Sens. Actuators B: Chem. 156 (2011) 395–400.
[19] T.H. Kwon, S.H. Park, J.Y. Ryu, H.H. Choi, Zinc oxide thin film doped with Al_2O_3, TiO_2 and V_2O_5 as sensitive sensor for trimethylamine gas, Sens. Actuators B: Chem. 46 (1998) 75–79.
[20] W.H. Zhang, W.D. Zhang, Fabrication of SnO_2–ZnO nanocomposite sensor for selective sensing of trimethylamine and the freshness of fishes, Sens. Actuators B: Chem. 134 (2008) 403–408.
[21] H.J. Kim, J.W. Yoon, K.I. Choi, H.W. Jang, A. Umar, J.H. Lee, Ultraselective and sensitive detection of xylene and toluene for monitoring indoor air pollution using Cr-doped NiO hierarchical nanostructures, Nanoscale 5 (2013) 7066–7073.
[22] Z. Lou, F. Li, J. Deng, L. Wang, T. Zhang, Branch-like hierarchical heterostructure (alpha-Fe_2O_3/TiO_2): a novel sensing material for trimethylamine gas sensor, ACS Appl. Mater. Interfaces 5 (2013) 12310–12316.
[23] N. Park, K. Sun, Z. Sun, Y. Jing, D. Wang, High efficiency NiO/ZnO heterojunction UV photodiode by sol–gel processing, J. Mater. Chem. C 1 (2013) 7333.
[24] J. Tian, Q. Zhang, L. Zhang, R. Gao, L. Shen, S. Zhang, X. Qu, G. Cao, ZnO/TiO_2 nanocable structured photoelectrodes for CdS/CdSe quantum dot co-sensitized solar cells, Nanoscale 5 (2013) 936–943.
[25] L. Xu, R. Zheng, S. Liu, J. Song, J. Chen, B. Dong, H. Song, NiO@ZnO heterostructured nanotubes: coelectrospinning fabrication, characterization, and highly enhanced gas sensing properties, Inorg. Chem. 51 (2012) 7733–7740.
[26] J. Zhai, D. Wang, L. Peng, Y. Lin, X. Li, T. Xie, Visible-light-induced photoelectric gas sensing to formaldehyde based on CdS nanoparticles/ZnO heterostructures, Sens. Actuators B: Chem. 147 (2010) 234–240.
[27] Z. Zhang, C. Shao, X. Li, C. Wang, M. Zhang, Y. Liu, Electrospun nanofibers of p-type NiO/n-type ZnO heterojunctions with enhanced photocatalytic activity, ACS Appl. Mater. Interfaces 2 (2010) 2915–2923.
[28] B. Zhao, G. Shao, B. Fan, W. Li, X. Pian, R. Zhang, Enhanced electromagnetic wave absorption properties of Ni–SnO_2 core–shell composites synthesized by a simple hydrothermal method, Mater. Lett. 121 (2014) 118–121.
[29] L. Lin, Y. Yang, L. Men, X. Wang, D. He, Y. Chai, B. Zhao, S. Ghoshroy, Q. Tang, A highly efficient TiO_2@ZnO n–p–n heterojunction nanorod photocatalyst, Nanoscale 5 (2013) 588–593.
[30] X. Hou, X. Wang, B. Liu, Q. Wang, Z. Wang, D. Chen, G. Shen, SnO_2@TiO_2 heterojunction nanostructures for lithium-ion batteries and self-powered UV photodetectors with improved performances, ChemElectroChem 1 (2014) 108–115.
[31] L. Huang, H. Fan, Room-temperature solid state synthesis of ZnO/α-Fe_2O_3 hierarchical nanostructures and their enhanced gas-sensing properties, Sens. Actuators B: Chem. 171–172 (2012) 1257–1263.
[32] C. Feng, S. Ruan, J. Li, B. Zou, J. Luo, W. Chen, W. Dong, F. Wu, Ethanol sensing properties of $LaCo_xFe_{1-x}O_3$ nanoparticles: effects of calcination temperature, co-doping, and carbon nanotube-treatment, Sens. Actuators B: Chem. 155 (2011) 232–238.
[33] R.S. Niranjan, M.S. Londhe, A.B. Mandale, S.R. Sainkar, L.S. Prabhumirashi, K. Vijayamohanan, I.S. Mulla, Trimethylamine sensing properties of thorium-incorporated tin oxide, Sens. Actuators B: Chem. 87 (2002) 406–413.
[34] W.-H. Zhang, W.-D. Zhang, Fabrication of SnO_2–ZnO nanocomposite sensor for selective sensing of trimethylamine and the freshness of fishes, Sens. Actuators B: Chem. 134 (2008) 403–408.
[35] X. Chu, S. Liang, T. Chen, Q. Zhang, Trimethylamine sensing properties of CdO–Fe_2O_3 nano-materials prepared using co-precipitation method in the presence of PEG400, Mater. Chem. Phys. 123 (2010) 396–400.
[36] X. Lu, Q. Yu, K. Wang, L. Shi, X. Liu, A. Qiu, L. Wang, D. Cui, Synthesis, characterization and gas sensing properties of flowerlike In_2O_3 composed of microrods, Cryst. Res. Technol. 45 (2010) 557–561.
[37] G. Korotcenkov, B.K. Cho, Instability of metal oxide-based conductometric gas sensors and approaches to stability improvement, Sens. Actuators B: Chem. 156 (2011) 527–538 (short survey).
[38] J. Wang, B. Zou, S. Ruan, J. Zhao, Q. Chen, F. Wu, HCHO sensing properties of Ag-doped In_2O_3 nanofibers synthesized by electrospinning, Mater. Lett. 63 (2009) 1750–1753.
[39] N. Barsan, U. Weimar, Conduction model of metal oxide gas sensors, J. Electroceram. 7 (2001) 143–167.
[40] Y.F. Sun, S.B. Liu, F.L. Meng, J.Y. Liu, Z. Jin, L.T. Kong, J.H. Liu, Metal oxide nanostructures and their gas sensing properties: a review, Sensors 12 (2012) 2610–2631.
[41] X.H. Liu, J. Zhang, X.Z. Guo, S.H. Wu, S.R. Wang, Enhanced sensor response of Ni-doped SnO_2 hollow spheres, Sens. Actuators B: Chem. 152 (2011) 162–167.
[42] P. Li, H.Q. Fan, Y. Cai, In_2O_3/SnO_2 heterojunction microstructures: facile room temperature solid-state synthesis and enhanced Cl_2 sensing performance, Sens. Actuators B: Chem. 285 (2013) 110–116.
[43] Y.B. Zhang, J. Yin, L. Li, L.X. Zhang, L.J. Bie, Enhanced ethanol gas-sensing properties of flower-like p-CuO/n-ZnO heterojunction nanorods, Sens. Actuators B: Chem. 202 (2014) 500–507.
[44] J.N. Deng, B. Yu, Z. Lou, L.L. Wang, R. Wang, T. Zhang, Facile synthesis and enhanced ethanol sensing properties of the brush-like ZnO–TiO_2 heterojunctions nanofibers, Sens. Actuators B: Chem. 184 (2013) 21–26.

Biographies

Chao Li received the bachelor degree in electronic science and technology from Jilin University, China in 2011. Now he is currently working for a doctor's degree and is mainly engaged in the research of functional nanomaterials and chemical sensors.

Caihui Feng received her PhD degree in the College of Electronic Science and Engineering, Jilin University, China in 2013. Now she is a post-doctor of College of Instrumentation and Electrical Engineering, Jilin University, and devoting herself to the research of sensors and detection technology.

Fengdong Qu received the bachelor degree from the College of Electronic Science and Engineering, Jilin University, China in 2012. Now, he is a graduate and engaged in the synthesis and characterization of the semiconducting functional materials and gas sensors.

Juan Liu received the bachelor degree from the College of Electronic Science and Engineering, Jilin University, China in 2012. Now, she is working for a master's degree and interested in functional materials and gas sensors.

Linghui Zhu received the bachelor degree from the College of Electronic Science and Engineering, Jilin University, China in 2011. She is currently studying for a doctor's degree and devoting herself to the research of functional nanomaterials, chemical sensors and photodetector.

Ying Lin received the bachelor degree from the College of Electronic Science and Engineering, Jilin University, China in 2012. Now, she is a graduate student and interested in functional materials and gas sensors.

Ying Wang received the bachelor degree from the College of Electronic Science and Engineering, Jilin University, China in 2013. Now, she is a graduate student and interested in functional materials and gas sensors.

Feng Li is an undergraduate in College of Electronic Science and Engineering, Jilin University, China, and interested in nanomaterials and chemical sensors.

Jingran Zhou received his PhD degree in the College of Electronic Science and Engineering, Jilin University, China in 2005. Now he is an assistant professor in the College of Electronics Science and Engineering, Jilin University, and interested in the field of characterizing and testing of the materials.

Shengping Ruan received the PhD degree in the College of Electronic Science and Engineering from Jilin University in 2001. Now, he is a full professor in the College of Electronics Science and Engineering, Jilin University, and mainly devoting himself to the research of electronic functional materials and devices.